Indian J. Phys. **71B** (1), 49–58 (1997)

I J P B
— an international journal

Analytical prediction of horseshoe chaos in a two coupled Duffing oscillators

S Rajasekar

Department of Physics, Manonmaniam Sundaranar University, Tirunelveli-627 002, Tamilnadu, India

and

S Paul Raj

Department of Physics, St. Xavier's College, Tirunelveli-627 002, Tamilnadu, India

Received 22 July 1996, accepted 14 October 1996

Abstract : A periodically driven two coupled Duffing oscillators is considered. The unperturbed system has homoclinic orbits. Onset of horseshoe chaos in the perturbed system is investigated using Melnikov-analytical technique. The nature of flow on the perturbed manifold is studied by an averaging procedure. The dimensionality of the stable and unstable manifolds of various fixed points of the averaged equations is studied. Then, analytical threshold condition for horseshoe chaos is obtained. The analytical prediction is found to be in good agreement with the numerical estimation of onset of chaos.

Keywords : Two coupled Duffing oscillators, chaos and Melnikov method

PACS No. : 05.45.+b

1. Introduction

The study of occurrence of chaotic behaviour in different parameter space of a nonlinear deterministic dynamical system is of great importance and this can be carried out using the numerical tools such as bifurcation diagram, Lyapunov exponents, power spectra analysis and so on. Such a computer based analysis requires large amount of time. However, for weakly perturbed systems the Melnikov method [1,2] is used for the prediction of horseshoe chaos analytically. In this paper, the homoclinic bifurcation in the two coupled Duffing oscillators

$$\ddot{x} = -d\dot{x} + A_1 x - \alpha_1 x^3 - \delta x y^2 + f\cos\omega t, \tag{1a}$$

$$\ddot{y} = -d\dot{y} + A_2 y - \alpha_2 y^3 - \delta x^2 y + f\cos\omega t, \tag{1b}$$

is studied using Melnikov method Eq. (1) has wide range of applications [3–8]. Recently, using Painlevé analysis we have identified the parametric choices for which the system (1) is integrable and constructed exact analytical solution for the integrable cases [9]

In general, to apply the Melnikov method the given equation of motion is rewritten in the standard form

$$\dot{X} = f(X) + \varepsilon g(X,t), \tag{2}$$

where $X = (x_1, x_2, \ldots, x_n)$, $f = (f_1, f_2, \ldots, f_n)$, $g = (g_1, g_2, \ldots, g_n)$ and g is periodic in t with period T. The unperturbed system of (2) should contain at least one saddle and centre fixed points and an integrable separatrix solution passing through the saddle point. In eq (1), if damping and forcing terms are chosen as the perturbations, then the unperturbed part is integrable [10,11] for four specific parametric choices only. Further, in one integrable case, the equations of motion were found to be separable and hence the choice is equivalent to the study of uncoupled Duffing oscillators. This has been noted earlier by Holmes and Marsden [12]. If the damping, coupling terms and external forces are treated as perturbations, then one can easily verify that the Melnikov function is independent of the parameter δ. Alternatively, in the present paper the subsystem

$$\dot{x} = A_1 x - \alpha_1 x^3 \quad \delta x y^2,$$

is considered as the unperturbed part. Accordingly, in the standard form of (2), eq. (1) can be written as

$$\dot{x}_1 = x_2, \tag{3a}$$

$$\dot{x}_2 = A_1 x_1 \quad \alpha_1 x_1^3 - \delta x_1 x_3^2 + \varepsilon(- d x_2 + f \cos\Theta), \tag{3b}$$

$$\dot{x}_3 = \varepsilon x_4, \tag{3c}$$

$$\dot{x}_4 = \varepsilon(A_2 x_3 \quad \alpha_2 x_3^3 - \delta x_1^2 x_3 - d x_4 + f \cos\Theta), \tag{3d}$$

$$\dot{\Theta} = \omega, \tag{3e}$$

where ε is a small parameter. In eq. (3), one oscillator is considered as weak compared to the other. Later, we show that the Melnikov function indeed depend on all the parameters of the system including δ.

The paper is organised as follows. In Section 2, first we study the nature of flow on the perturbed manifold by an averaging procedure. The dimensionality of the stable and unstable manifolds of various fixed points of the averaged equations is studied. Then, analytical threshold condition for horseshoe chaos is obtained. In Section 3, analytical prediction is compared with numerical results. Finally, Section 4, contains summary and conclusions.

2. Calculation of Melnikov function

The Melnikov analysis starts with the identification of saddle fixed point and separatrix solution in the unperturbed system. The fixed points of (3) with $\varepsilon = 0$ are $x_1(x_3)$, $x_2 = 0$, $x_3(x_4)$, where $x_1(x_3)$ is the roots of the equation

$$x_1(A_1 - \alpha_1 x_1^2 - \delta x_3^2) = 0 \tag{4}$$

and x_3, x_4 are arbitrary. The roots of (4) are

$$x_1 = 0, \pm [(A_1 - \delta x_3^2)/\alpha_1]^{1/2}. \tag{5}$$

For $x_3 \in (-\sqrt{A_1/\delta}, \sqrt{A_1/\delta})$, there are three real roots with intermediate root corresponding to a hyperbolic and the other two are elliptic fixed points. For $|x_3| > \sqrt{A_1/\delta}$, there exists only one elliptic fixed point $(0, 0, x_3, x_4)$. For $|x_3| < \sqrt{A_1/\delta}$, the fixed point $\phi(0, 0, x_3, x_4)$ is connected to itself by a pair of homoclinic orbits which satisfy

$$\frac{1}{\gamma}\left[x_2^2 - A_1 x_1^2 + (\alpha_1/2)x_1^4 + \delta x_1^2 x_3^2\right] = 0. \tag{6}$$

The phase space of (3) appears as in Figure 1, where the component x_4 is suppressed for clarity. The entire picture holds for any value of x_4. The unperturbed system has hyperbolic

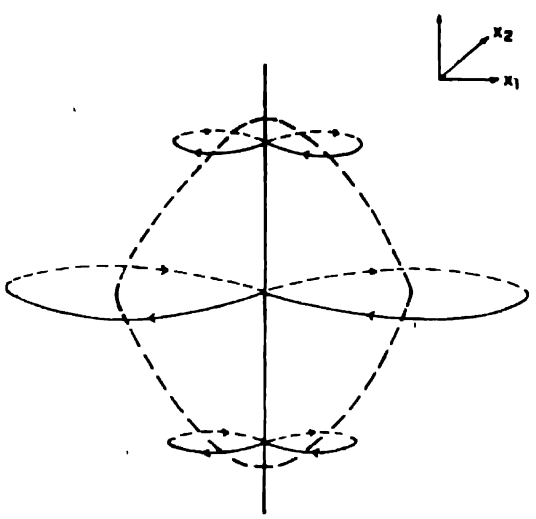

Figure 1. Homoclinic orbits of the unperturbed system (3) ($\varepsilon = 0$). Solid verticle line and solid dotted curve represents the solution of (4).

invariant manifold M with boundary $\phi(x_1(x_3), 0, x_3, x_4, \Theta_0)$, where $x_3 \in (-\sqrt{A_1/\delta}, \sqrt{A_1/\delta})$ and $\Theta_0 \in (0, 2\pi/\omega)$.

In the perturbed system, assume that M persists as invariant manifold M_ε given by

$$M_\varepsilon = (\phi(x_1(x_3)), 0, x_3, x_4) + \sigma(\varepsilon, \Theta_0). \tag{7}$$

In the unperturbed system, $x_3 = x_4 = 0$ and hence the manifold M is invariant and therefore, no orbits cross the boundary. In the perturbed system, x_3 and x_4 need not be zero so all orbits may leave the perturbed manifold by crossing the boundary. In this case, the nature of stable and unstable manifolds in the perturbed system and the significances of transverse intersections of stable and unstable manifolds are not well understood [2]. However, the presence of orbits homoclinic to fixed points and periodic orbits have dramatic dynamical consequences. In particular, the homoclinic orbits can provide the mechanism for the folding of the phase space. Further, the invariant sets such as fixed points and periodic orbits to which the orbit is homoclinic, can provide the mechanism for the stretching and contraction which are essential for producing chaotic motion. Thus, it is necessary to know the flow on the normally hyperbolic manifold M_ε under the perturbation. The nature of flow on the perturbed M_ε can be studied by the averaging procedure. If periodic orbits exist on M_ε, then the appropriate Melnikov integral can be computed to determine whether or not the stable and unstable manifolds of the periodic orbits intersect transversely. Thus, the next step is to determine whether M_ε contains any periodic orbits. For this purpose, we consider the perturbed equations restricted to M_ε given by eqs. (3c–3e). Periodic orbits of (3c–3e) in a suitable Poincaré surface of section or Poincaré map become a fixed point. So, we consider the averaged equations

$$\dot{x}_3 = (\varepsilon / 2\pi) \int_0^{2\pi} x_4 d\Theta = \varepsilon x_4, \tag{8a}$$

$$\dot{x}_4 = (\varepsilon / 2\pi) \int_0^{2\pi} (-d x_4 + A_2 x_3 - \alpha_2 x_3^3 - \delta x_1^2 x_3 + f \cos\Theta) d\Theta$$

$$= \varepsilon(-d x_4 + A_2 x_3 - \alpha_2 x_3^3 - \delta x_1^2 x_3). \tag{8b}$$

The fixed points of the averaged eq. (8) corresponds to the periodic orbits of (3c–3e) of period $2\pi/\omega$, having the same stability type as the fixed points of the averaged equations. Further, the periodic orbits on M_ε become fixed points of the four dimensional Poincaré map of eq. (3) formed by fixing $\Theta = \Theta$ $(= 2\pi/\omega)$. The fixed points of the averaged equations are $(x_3, x_4) = (0, 0)$, $(\pm\sqrt{I}, 0)$, where $I = (A_2 - \delta x^2)/\alpha_2$. When $x_1 = 0$, we obtain $I = A_2/\alpha_2$. The stability determining eigenvalues are obtained from

$$\lambda^2 + \varepsilon d\lambda - \varepsilon^2(A_2 - 3\alpha_2 x_3^2 - \delta x_1^2 - 2\delta x_1 x_3 (dx_1 / dx_3)) = 0. \tag{9}$$

dx_1/dx_3 can be obtained from eq. (4). From eq. (9), we found that the Poincaré map has the following structure :

(i) $d^2 > 8A_2$:

The fixed point $(x_1, x_2, x_3, x_4) = (0, 0, 0, 0)$ has a two dimensional stable and two dimensional unstable manifolds. The fixed points $(0, 0, \pm\sqrt{I}, 0)$ are of saddle-node type. They have one dimensional unstable and three dimensional stable manifolds.

(ii) $d^2 < 8A_2$:

The saddle point $(0, 0, 0, 0)$ has a two dimensional stable and two dimensional unstable manifolds. The fixed points $(0, 0, \pm\sqrt{I}, 0)$ are saddle-focus and possess three dimensional stable manifolds (spiralling in the x_3, x_4 directions) and one dimensional unstable manifolds.

Figure 2 shows the geometry of the Poincaré map where the coordinate x_2 is suppressed for clarity.

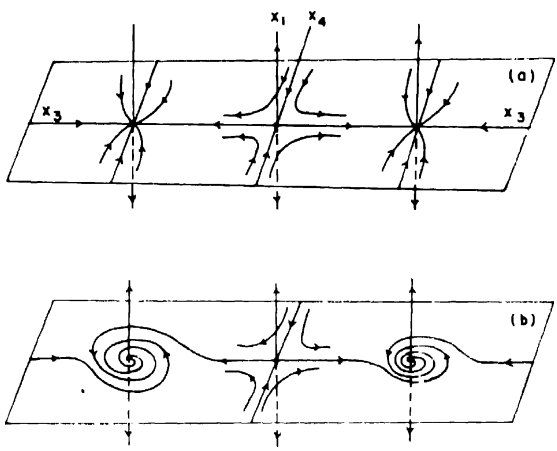

Figure 2. The geometry of the Poincaré map in a three dimensional phase space by ignoring the one dimension of the state manifold for (a) $d^2 > 8A_2$ and (b) $d^2 < 8A_2$

For the system of the form

$$\begin{aligned}
\dot{x}_1 &= f_1(x_1, x_2, y_1, y_2) + \varepsilon g_1(x_1, x_2, y_1, y_2, t), \\
\dot{x}_2 &= f_2(x_1, x_2, y_1, y_2) + \varepsilon g_2(x_1, x_2, y_1, y_2, t), \\
\dot{y}_1 &= \varepsilon G_1(x_1, x_2, y_1, y_2, t), \\
\dot{y}_2 &= \varepsilon G_2(x_1, x_2, y_1, y_2, t),
\end{aligned} \tag{10}$$

the Melnikov function is given by [2]

$$\begin{aligned}
M(t_0) = \int_{-\infty}^{\infty} [&< D_X H(X, Y), g > + < D_Y H(X, Y), G >] (X(\tau), Y, \tau) d\tau \\
&- < D_Y (X(Y), Y), \int G(X, Y, \tau) d\tau >,
\end{aligned} \tag{11}$$

where D_Z denotes differentiation with respect to Z, $X = (x_1, x_2)$, $Y = (y_1, y_2)$, H is the hamiltonian of the unperturbed system and $\bar{Y}$ is the fixed point of the averaged eq. (8). Here, $< f, g >$ represents inner product of f and g. The homoclinic trajectories of the unperturbed system of (3) are given by the following analytical expressions.

Case 1. $(x_3, x_4) = (0, 0)$:

$$x_{1h}(\tau) = \pm\sqrt{2A_1\alpha_1}\,\mathrm{sech}\sqrt{A_1}\,\tau, \tag{12a}$$

$$x_{2h}(\tau) = \mp\sqrt{2/\alpha_1}\,A_1\,\mathrm{sech}\sqrt{A_1}\,\tau\tanh\sqrt{A_1}\,\tau. \tag{12b}$$

Case 2. $(x_3, x_4) = (\pm\sqrt{I}, 0)$:

$$x_{1h}(\tau) = \pm\sqrt{2(A_1 - \delta I)/\alpha_1}\,\mathrm{sech}\sqrt{(A_1 - \delta I)}\,\tau, \tag{13a}$$

$$x_{2h}(\tau) = \mp\sqrt{2/\alpha_1}\,(A_1 - \delta I)\,\mathrm{sech}\sqrt{(A_1 - \delta I)}\,\tau\,\tanh\sqrt{(A_1 - \delta I)}\,\tau. \tag{13b}$$

Using the homoclinic orbits (12) and (13) in (11) and evaluating the integral, we find

Case 1. $(x_3, x_4) = (0, 0)$:

$$M(t_0) = [-4dA_1^{3/2}/(3\alpha_1)] \pm f\pi\omega\sqrt{2/\alpha_1}\,\mathrm{sech}(\pi\omega/(2\sqrt{A_1}))\sin\omega t_0. \tag{14}$$

Case 2. $(x_3, x_4) = (\pm\sqrt{I}, 0)$:

$$M(t_0) = A + f(B\cos\omega t_0 \pm C\sin\omega t_0), \tag{15a}$$

where

$$A = 4(A_1 - \delta I)^{3/2}[-d\alpha_1 - 4\delta^2 I + 3\delta I\alpha_1(A_2 - \alpha_2 I)/(A_1 - \delta I)]/(3\alpha_1^2),$$

$$B = [\delta\sqrt{I}\,\pi\omega\,\mathrm{cosech}(\pi\omega/(2\sqrt{A_1 - \delta I}))]/\alpha_1,$$

$$C = [\sqrt{2}\,\pi\omega\,\mathrm{sech}(\pi\omega/(2\sqrt{A_1 - \delta I}))]/\alpha_1. \tag{15b}$$

The case $(x_3, x_4) = (0, 0)$ corresponds to the uncoupled Duffing oscillator [1]. Now we shall analyse the Case 2. The necessary condition for the intersection of stable and unstable orbits is obtained as

$$f \geq f_M = |A|/\sqrt{B^2 + C^2}. \tag{16}$$

The sufficient condition requires the existence of simple zeros of $M(t_0)$. For $f > f_M$, $M(t_0)$ oscillates between positive and negative values indicating that the stable and unstable manifolds intersect transversely producing local chaos. The value of f_M corresponds to the homoclinic tangency The prediction of f_M from eq. (16), is plotted in Figure 3 in (ω, f) parameter space. Horseshoe chaos occurs in the region above the threshold curve.

3. Numerical simulations

In general, the existence of horseshoe does not imply that the typical trajectories will be asymptotically chaotic. However, it can exert a dramatic influence on the behaviour of

orbits which pass close to it. In many dynamical systems, the presence of horseshoe was shown to be the starting point over which the systems undergone some of the possible routes to chaos. Consequently, the Melnikov threshold curve is considered as a lower

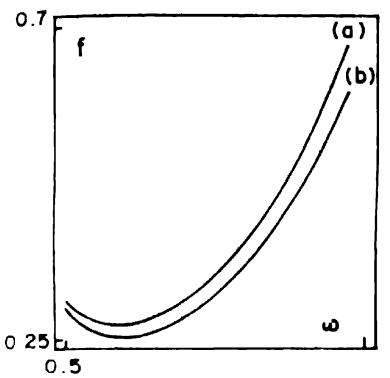

Figure 3. Threshold curves for horseshoe chaos in the (ωf) plane for $\alpha_1 = 1$, $\alpha_2 = 0.1$, $A_1 = 1$, $A_2 = 0.11$, $d = 0.4$ and (a) $\delta = 0.1$ and (b) $\delta = 0.05$

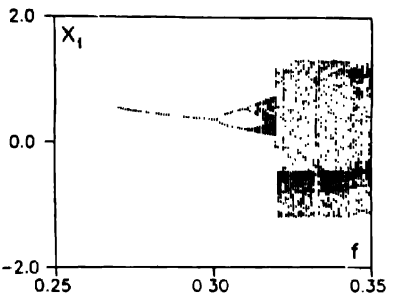

Figure 4. Bifurcation diagram as a function of f for $\omega = 1$ and $\delta = 0.1$ for the coupled oscillators

threshold for the onset of asymptotic chaos. In view of this, we have numerically investigated the onset of chaos in eq. (3). For $\delta = 0.1$, the Melnikov threshold value f_M is 0.305. The other parameters values are fixed as $d = 0.4$, $\alpha_1 = 1$, $\alpha_2 = 0.1$, $A_1 = 1$, $A_2 = 0.11$ and $\omega = 1.0$. Figure 4 shows the bifurcation phenomenon as a function of the parameter f.

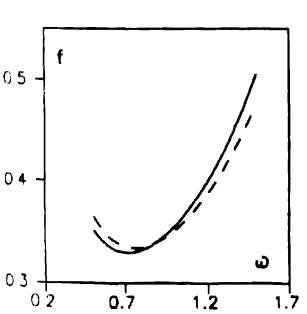

Figure 5. Melnikov threshold curves for the coupled systems (continuous curve) for $\delta = 0.1$ and uncoupled system (dashed curve).

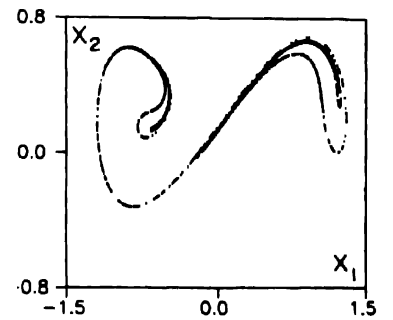

Figure 6. Poincaré map of the chaotic attractor of the uncoupled system at the onset of chaos.

Period doubling phenomenon leading to chaotic motion is found to occur when the parameter f is varied from small value. We denote f_c as the critical value of the parameter f,

at which onset of chaos where trajectory jumps between positive and negative values of x_1 and x_3, occurs. Numerically, the onset of chaos is found to occur at $f_c \approx 0.32$.

To know the influence of the second oscillator (3c–3d) on the onset of chaotic dynamics of the coupled Duffing oscillators, we have studied the onset of chaos in the uncoupled Duffing oscillator

$$= x_3 \tag{17a}$$

$$\dot{x}_2 = A_1 x_1 - \alpha_1 x^3 - \varepsilon(-dx_2 + f\cos\Theta). \tag{17b}$$

In eq. (17) the parameter values are fixed at $A_1 = 1$, $\alpha_1 = 1$, $d = 0.4$ and $\omega = 1$, the same as those used in the coupled oscillators. Figure 5 shows the threshold curves for the onset of chaos in both the uncoupled and coupled oscillators. The continuous and dashed curves represent f_M for the coupled and uncoupled systems, respectively. From this figure, we note

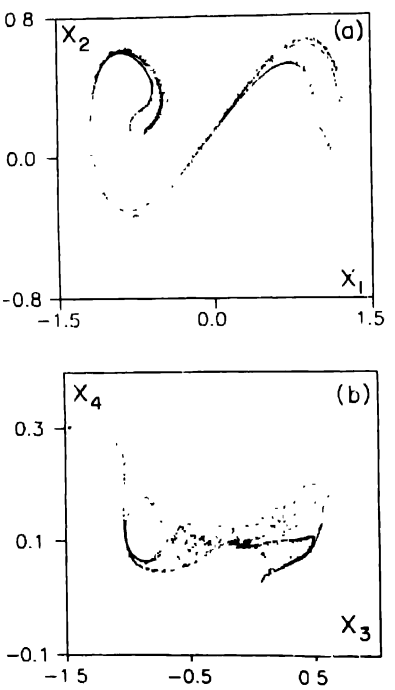

Figure 7. Chaotic attractor of the coupled oscillators.

that for ω less than a critical value ω_c, the f_M of the coupled oscillators is lower than the uncoupled system. However for $\omega > \omega_c$, the f_M value of the coupled system is higher than that of the uncoupled systems. This is further varified by numerical experiment. In the uncoupled oscillators, onset of chaos is found at $f_c = 0.307$ ($f_M = 0.3013$). This f_c value can

be compared with the value $f_c = 0.32$ of the coupled oscillators. That is, onset of chaos is delayed in the coupled oscillators. In the uncoupled system, also period doubling bifurcation culminating in chaos is observed.

The nature of the chaotic attractor at f_c is also studied in the coupled and uncoupled oscillators. Figure 6 shows the Poincaré map of the chaotic attractor at $f_c = 0.307$ for the uncoupled system. Figure 7 shows the attractor of the coupled systems for $f_c = 0.32$. The influence of the coupling term and second oscillator on the structure of the chaotic attractor can be clearly seen. In the uncoupled system, chaotic attractor consists of thin layer structures. The geometrical structure of the attractors of both the coupled and uncoupled systems, appear almost similar. However, in the coupled systems due to the coupling term, the points in the x_1–x_2 plane are distributed in the neighbourhood of the layers. On the other hand, the geometrical structure of the coupled systems in the x_3–x_4 plane is highly different. This is due to the small values of the parameters of the second oscillator. A detailed analysis of the prediction of onset of chaos has been formed for different sets of ω and d. The results are summarized in Table 1. From this table, the analytical prediction is found to

Table 1. Critical values of f_M and f_c for various values of d and ω for the coupled Duffing oscillators.

		f_M	f_c
1.0	0.25	0.201	0.237
	0.30	0.236	0.245
	0.35	0.271	0.278
	0.40	0.305	0.320
	0.45	0.341	0.350
1.5	0.40	0.451	0.580
1.8	0.40	0.631	0.705
2.0	0.40	0.760	0.810

be in good agreement with the numerical analysis of the system. Since the second oscillator is treated as weak, the present analysis is applicable for small values of A_2, α_2, δ, d and f.

4. Summary and conclusions

In this paper, we have applied Melnikov-analytical technique to a two coupled Duffing oscillators to predict onset of chaos. Even though the scaling of eq. (3) seems to be artificial, it is done in order to obtain the Melnikov function in terms of all the parameters including δ. Interestingly, the calculated Melnikov function indeed depend on all the parameters of the system which clearly justifies the scaling introduced in (3). The influence of the second oscillator (3c–3d) on the onset of chaotic dynamics of the coupled Duffing oscillators, has also been studied. The analytical prediction is found to be in good agreement with the numerical onset of chaos in the two coupled Duffing oscillators.

Acknowledgment

The present work forms part of the University Grants Commission, minor research project of the author SR.

References

[1] J Guckenheimer and P Holmes *Nonlinear Oscillations, Dynamical System and Bifurcation of Vector Fields* (Berlin Springer-Verlag) (1983)

[2] S Wiggins *Global Bifurcations and Chaos* (New York : Springer-Verlag) (1988)

[3] J A Elliott *Am J Phys* **50** 1148 (1982)

[4] M A F Sanjuan, J L Valero and M G Velarde *Nuovo Cim* **13** 913 (1991)

[5] S A Nayfeh and A H Nayfeh *Int J Bifur Chaos* **3** 417 (1993)

[6] T A Nayfeh and A F Vakakis *Int J Nonl Mech* **29** 233 (1994)

[7] R Nabergoj, A Tondl and Z Virag *Chaos, Solitons and Fractals* **4** 263 (1994)

[8] F C Moon *Chaotic Vibrations* (New York Wiley-Interscience) (1987)

[9] S Rajasekar and S Paul Raj *Pramana-J Phys* **47** 183 (1996)

[10] M Lakshmanan and R Sahadevan *Phys Rev* **A31** 861 (1985)

[11] G Baumann, W G Glockle and T F Nonnenmacher *Proc Roy Soc London* **A434** 263 (1991)

[12] P Holmes and J Marsden *Archieve for Rati Mech Anal* **76** 135 (1981)